Title

R–MDDMA is a Safer Analogue of MDMA with Therapeutic Potential

Journal

ACS Chemical Neuroscience

ISSN

1948-7193

Authors

Vargas, MaxemilianoV

Hatzipantelis, Cassandra J

Dunlap, Lee E

et al.

Publication Date

2026-04-20

DOI

10.1021/acschemneuro.5c00891

ACS Chemical Neuroscience

pubs.acs.org/chemneuro Research Article

R-MDDMA is a Safer Analogue of MDMA with Therapeutic Potential

Maxemiliano V. Vargas, Cassandra J. Hatzipantelis, Lee E. Dunlap, Robert J. Tombari, Arabo A. Avanes, Sam Vaillancourt, Pierre Llorach, Juliana S. Salgado, Boris D. Heifets, and David E. Olson*

Cite This: *ACS Chem. Neurosci.* 2026, 17, 1670−1682 Read Online

ACCESS | Metrics & More | Article Recommendations

ABSTRACT: Recent clinical evidence suggests that racemic 3,4-methylenedioxymethamphetamine (MDMA) might be useful for treating a range of neuropsychiatric diseases including post-traumatic stress disorder (PTSD) and depression. However, concerns about its abuse potential stemming from its monoamine releasing properties have hampered its clinical development. Thus, safer analogues of racemic MDMA with comparable therapeutic effects are highly desirable. Here, we compare the pharmacological effects of MDMA enantiomers with those of its methylated analogue 3,4-methylenedioxy-*N*,*N*-dimethylamphetamine (MDDMA). We found that *R*-MDDMA did not directly activate 5-HT2B receptors, induce serotonin efflux, produce a head-twitch response, impact body temperature, or induce hyperlocomotion at therapeutically relevant doses. However, it still promoted structural neuroplasticity in cortical neurons, facilitated fear extinction learning, and produced sustained antidepressant-like effects. Taken together, our results suggest that *R*-MDDMA might be a safer MDMA analogue with similar therapeutic properties.

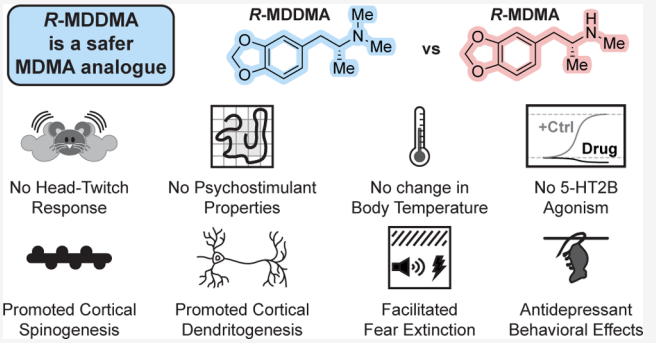

KEYWORDS: *MDMA, entactogen, MDDMA, psychoplastogen, PTSD, depression, psychedelic*

INTRODUCTION

Racemic 3,4-methylenedioxymethamphetamine (*R*,*S*-MDMA) is a substituted phenethylamine with structural similarities to both psychostimulants and psychedelics.[1] It was first described and synthesized in a German patent issued to Merck in 1912 and largely forgotten until the late 1970s when it was rediscovered by Alexander Shulgin and demonstrated to possess therapeutic potential when used in talk therapy.[2,3] Despite being listed as a schedule 1 controlled substance, interest in *R*,*S*-MDMA as a therapeutic has persisted. In preclinical models *R*,*S*-MDMA facilitates fear extinction learning and promotes prosocial behaviors.[4−8] Moreover, several clinical trials have demonstrated its efficacy for addressing the symptoms of post-traumatic stress disorder (PTSD) with high patient response rates.[9−11] However, the U.S. Food and Drug Administration (FDA) recently denied a New Drug Application (NDA) to use *R*,*S*-MDMA in conjunction with psychotherapy due to concerns about abuse potential among other issues.[12] More recently, others have studied *R*,*S*-MDMA in the context of treating major depressive disorder (MDD).[13]

Despite the many issues that make the clinical development of *R*,*S*-MDMA challenging, its therapeutic potential remains high. Its safety profile is suboptimal, and its pharmacology suggests that it may have abuse potential.[1] Similar to other para-substituted amphetamines, *R*,*S*-MDMA interacts with the serotonin transporter (SERT), dopamine transporter (DAT), and norepinephrine transporter (NET) leading to an increase in extracellular monoamine concentrations.[1,14] Its monoamine releasing properties, particularly its effects on dopamine release, endow it with psychostimulant-like qualities and mediate its acute reinforcing effects in rodents and other species.[15−17] However, the effects of *R*,*S*-MDMA on serotonin release through SERT and subsequent serotonin receptor activation are largely thought to be responsible for its prosocial effects and enhancement of fear extinction learning,[18,19] and might constrain its addictive potential.[20]

While most research has focused on *R*,*S*-MDMA, each enantiomer has been shown to exhibit unique pharmacology.[1] Howell and co-workers demonstrated that *S*-MDMA (Figure 1) is primarily responsible for the monoamine releasing properties and abuse potential of the racemic mixture, while *R*-MDMA lacks potent dopamine releasing properties yet is still able to elicit prosocial effects and facilitate fear extinction

Received: November 11, 2025
Revised: April 9, 2026
Accepted: April 14, 2026
Published: April 21, 2026

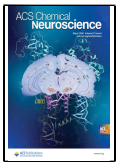

https://doi.org/10.1021/acschemneuro.5c00891
ACS Chem. Neurosci. 2026, 17, 1670−1682

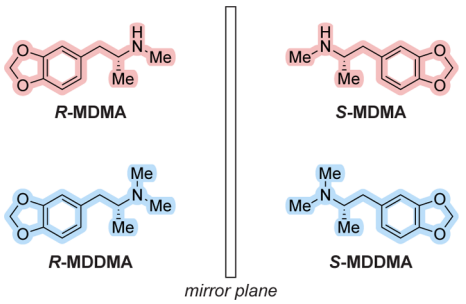

Figure 1. Structures of MDMA and MDDMA enantiomers. The structures of *R*-MDMA and *R*-MDDMA are shown separated from *S*-MDMA and *S*-MDDMA by a mirror plane. The enantiomers of MDMA and MDDMA are highlighted in red and blue, respectively.

learning in preclinical rodent models.[21,22] Similarly, Heifets and co-workers have found *R*-MDMA to possess therapeutic properties with lower abuse potential than the racemic mixture.[20]

Despite the importance of serotonin release in mediating some of the biological effects of *R,S*-MDMA, it does not represent the totality of the drug's relevant pharmacological activity. For example, serotonin release alone is insufficient to promote the enhancement of fear extinction learning, as demonstrated by the inability of fenfluramine to promote fear extinction.[18] Moreover, many studies have demonstrated that racemic MDMA and its enantiomers bind a variety of neuroreceptors including 5-HT2A, 5-HT2B, trace amine-associated receptor 1 (TAAR1), among others, albeit with low affinities.[1] Our lab has demonstrated that *R,S*-MDMA is a potent psychoplastogen[23,24] capable of promoting structural neuroplasticity in rat cortical cultures via a 5-HT2-dependent mechanism.[25] Furthermore, there is evidence that *R,S*-MDMA leads to upregulation of brain-derived neurotropic factor (BDNF) in the frontal cortex of mice,[26] suggesting a potential mechanism through which cortical plasticity could lead to therapeutic effects such as accelerated fear-extinction learning.[27]

Our interest in developing safer analogues of *R,S*-MDMA that might also be used to probe its therapeutic mechanisms led us to investigate racemic 3,4-methylenedioxy-*N,N*-dimethylamphetamine (*R,S*-MDDMA). This compound was originally synthesized by Alexander Shulgin and described as an MDMA analogue lacking the psychostimulant properties of its parent compound.[28] A recent study examining the properties of MDMA analogues at monoamine transporters demonstrated that *R,S*-MDDMA retained some activity as a serotonin releaser, while its ability to serve as a monoamine releaser through DAT or the norepinephrine transporter NET was greatly reduced compared to *R,S*-MDMA.[29] We hypothesized that the remaining SERT activity was likely due to the *S*-enantiomer and that *R*-MDDMA might be an MDMA analogue lacking monoamine transporter activity (Figure 1). Moreover, we hoped that *R*-MDDMA might be a potent psychoplastogen given that increasing *N*-methylation tends to improve cellular membrane penetrance and enables stimulation of intracellular 5-HT2A receptors leading to cortical neuron growth.[30] Here, we compare the pharmacological effects of *R*-MDDMA to those of *R*-MDMA.

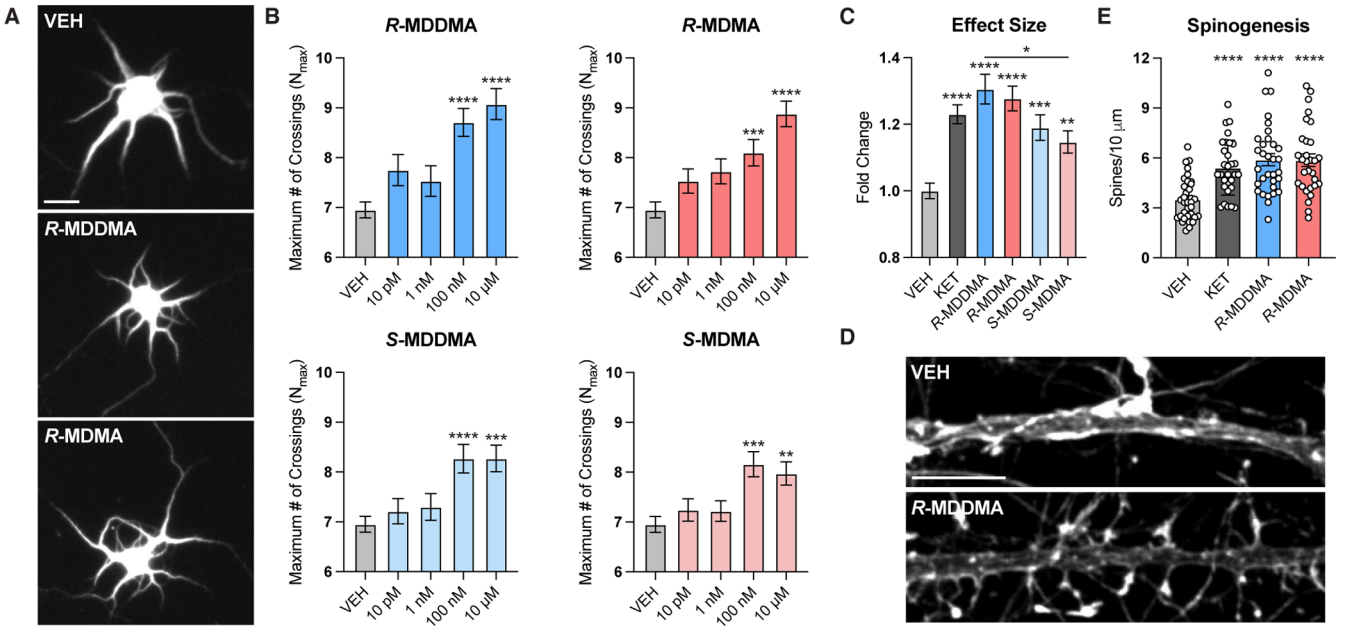

Figure 2. *R*-MDDMA promotes cortical neuron growth. (A) Representative widefield images of cortical neurons (DIV6) treated with MDDMA and MDMA enantiomers for 72 h. Both MDDMA and MDMA enantiomers increase dendritic arborization relative to the vehicle control. Scale bar = 20 μm. (B) Maximal number of crossings (N_{max}) from Sholl plots (N = 47−103 neurons from two independent cultures). (C) Effect sizes relative to the VEH control of compounds treated at 10 μM. (D) Representative confocal images of DIV15 cortical neurons treated for 24 h with 1 μM *R*-MDDMA and *R*-MDMA. (N = 30−37 neurons from two independent cultures). Scale bar = 5 μm. (E) Both *R*-MDDMA (1 μM) and *R*-MDMA (1 μM) increase dendritic spine density on cortical neurons (DIV15) after treatment for 24 h. Data represent mean ± SEM ****p < 0.0001, ***p < 0.001, **p < 0.01, *p < 0.05. One-way ANOVA with Dunnett's (B and E, compared to VEH) or Tukey's (C, compared to VEH unless noted with a bar) multiple comparisons tests (B, *R*-MDDMA $F(5, 444) = 11.03$; B, *R*-MDMA $F(5, 443) = 11.41$; B, *S*-MDDMA $F(5, 423) = 9.581$; B, *S*-MDMA $F(5, 481) = 9.995$; C, $F(5, 447) = 12.86$; E, $F(3, 125) = 14.37$. VEH = vehicle (0.1% DMSO); KET = ketamine.

https://doi.org/10.1021/acschemneuro.5c00891
ACS Chem. Neurosci. 2026, 17, 1670−1682

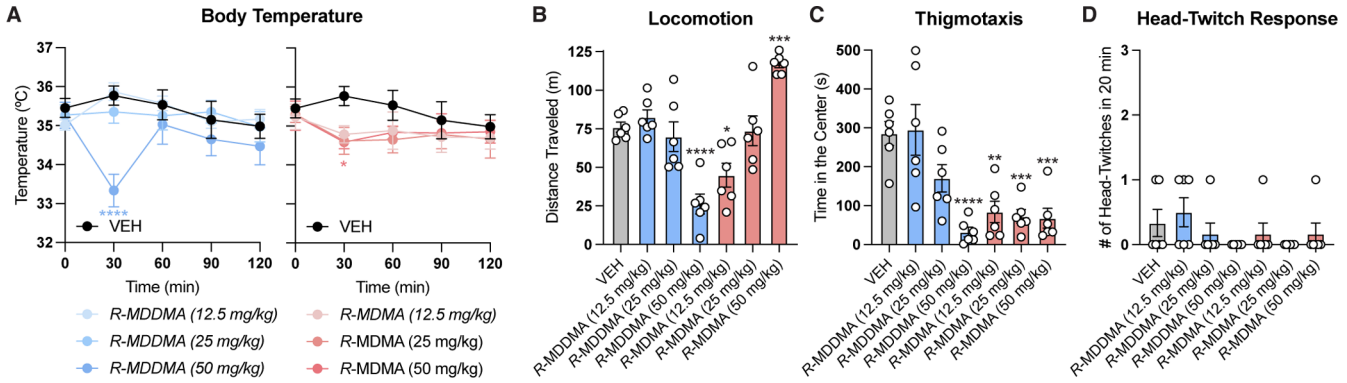

Figure 3. *R*-MDDMA does not induce hyperthermia, hyperlocomotion, or a head-twitch response. (A) C57BL/6J mice were treated with *R*-MDDMA or *R*-MDMA via intraperitoneal (IP) injections and temperature was measured using an infrared thermometer every 30 min for 2 h. N = 6 mice (3 males and 3 females) per treatment group. (B,C) The same mice dosed in A were placed in a novel arena immediately after treatment, and total distance as well as time spent in the center of the arena were measured for 30 min, prior to the first postcompound temperature measurement. (D) During the first 20 min in the novel area the mice were video recorded, and the number of head-twitches was manually quantified by a blinded observer. Data represent mean ± SEM ****p < 0.0001, ***p < 0.001, **p < 0.01, *p < 0.05. Two-way ANOVA with Dunnett's multiple comparisons test (C, comparing each dose to the VEH control for the time point) or a one-way ANOVA with Dunnett's multiple comparisons tests (B, C, D, compared to VEH) (A, interaction F (12, 100) = 2.031, time F (4, 100) = 1.085, treatment F (3, 100) = 6.680; B, F (6, 35) = 17.73; C, F (6, 35) = 9.937; D, F (6, 35) = 1.250. VEH = vehicle (0.9% saline).

RESULTS AND DISCUSSION

R-MDDMA Promotes Cortical Neuron Growth

Previously, we demonstrated that *R,S*-MDMA promotes the growth of E18 rat cortical neurons in culture, and this effect was blocked by the 5-HT2 antagonist ketanserin (KETSN).[25] Presumably, *R,S*-MDMA mediates this effect by acting directly on 5-HT2 receptors, as E18 embryonic rat cortical neurons do not express SERT[31] and serotonin cannot promote the growth of these neurons in culture.[25,30] As the structural neuroplasticity-promoting effects of *R,S*-MDMA, psychedelics, ketamine, and other psychoplastogens may underlie their sustained therapeutic effects,[24] we were interested in determining if the enantiomers of MDMA and MDDMA produced differential effects on cortical neuron growth.

First, we treated cultures prepared from E18 embryonic rat cortex with increasing concentrations of *R*- and *S*-enantiomers of MDMA and MDDMA and assessed the complexity of the dendritic arbors at 6 days in vitro (DIV6) using Sholl analysis (Figure 2A−C) as described previously.[32] All compounds produced a concentration-dependent increase in the maximum number of crossings (N_{max}) of the Sholl plots with effects emerging in the nanomolar range (Figure 2B). At the highest concentration tested (10 μM), all compounds, as well as the positive control (ketamine) produced statistically significant increases in dendritic arborization relative to the vehicle control (Figure 2C). However, *R*-MDDMA exhibited the greatest effect size, though its effect size was only statistically different than that of S-MDMA (p = 0.0238).

To determine the effects of *R*-MDDMA and *R*-MDMA on more mature cortical cultures (15 days in vitro, DIV15), we assessed spine density following 24 h of treatment. Both *R*-MDDMA and *R*-MDMA (1 μM) increased spine density to a comparable extent as the positive control (10 μM ketamine) (Figure 2D,E). Taken together, these results suggest that *R*-MDDMA is a potent psychoplastogen and inducer of cortical neuron growth, with effects comparable to *R*-MDMA.

R-MDDMA Does Not Induce Effects Characteristic of Psychostimulants or Psychedelics

Given that *R,S*-MDMA and other psychostimulants are known to induce hyperthermia that can be life-threatening under certain conditions,[33] we first tested the impact that increasing doses of *R*-MDMA and *R*-MDDMA had on core body temperature (Figure 3A). We chose three doses (12.5 mg/kg, 25 mg/kg, and 50 mg/kg) of both compounds with the middle dose being 25 mg/kg based on previous studies by Howell and co-workers demonstrating that 17 mg/kg of *R*-MDMA produces therapeutic effects without the characteristic psychostimulant and hyperthermic responses induced by *R,S*-MDMA.[22] We found that neither *R*-MDMA nor *R*-MDDMA increased body temperature at any dose over the course of 2 h. However, the high dose (50 mg/kg) of both drugs led to a transient decrease in body temperature at the 30 min time point that resolved within 30 min (Figure 3A).

To assess psychostimulant-like effects commonly associated with DAT inhibitors and dopamine releasers,[34,35] we performed novelty-induced locomotion (NIL) assays. At the low dose (12.5 mg/kg) *R*-MDMA decreased locomotion, but it increased locomotion at the highest dose tested (50 mg/kg) (Figure 3B). This indicates that *R*-MDMA might possess weak dopaminergic activity with the risk for abuse if used at sufficiently high doses and aligns with a recent clinical study suggesting that *R*-MDMA might simply be less potent than *S*-MDMA without major qualitative differences between the drugs.[38] Moreover, *R*-MDMA produced a strong anxiety-like response, with all doses tested leading to significantly less time spent in the center of the arena (Figure 3C). In stark contrast, *R*-MDDMA did not produce any statistically significant changes in locomotion or thigmotaxis at the low and medium doses tested (12.5 mg/kg and 25 mg/kg, respectively) (Figure 3B,C). However, the 50 mg/kg dose of *R*-MDDMA decreased locomotion and increased thigmotaxis.

At higher doses, *R,S*-MDMA has been described to be weakly hallucinogenic producing simple visual distortions described as flashes of light in the peripheral visual field.[36] To test for the possibility of psychedelic-like properties, we examined video recordings of mice in the open field

https://doi.org/10.1021/acschemneuro.5c00891
ACS Chem. Neurosci. 2026, 17, 1670−1682

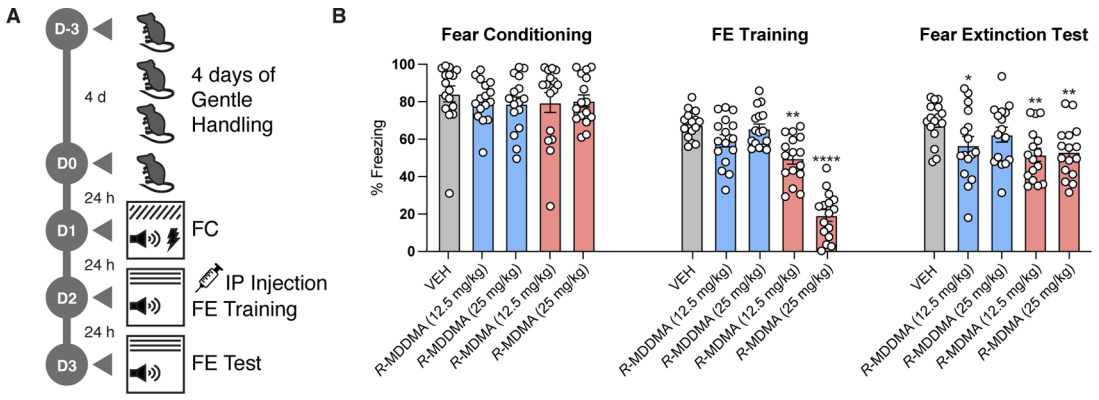

Figure 4. *R*-MDDMA facilitates fear extinction learning. (A) Schematic depicting experimental design. Following cued fear conditioning, C57BL/6J mice were treated with *R*-MDDMA or *R*-MDMA via intraperitoneal (IP) injections and subjected to cued fear extinction training. Fear extinction memory was assessed 24 h later. The fear conditioning procedure consisted of six pairings of an auditory cue (80−85 dB white noise, 15 s) coterminating with a foot shock (0.85 mA and 2 s), each spaced 1.5 min apart. $N = 16$ mice (8 males and 8 females) per treatment group. Note: none of the groups received compounds prior to fear conditioning, but the labels are used to associate groups with their respective future treatments. (B) Treatment with *R*-MDDMA (12.5 mg/kg) and *R*-MDMA (12.5 and 25 mg/kg) prior to fear extinction (FE) training led to a sustained reduction in freezing behavior measured 24 h later upon reactivation of the cued fear memory. Data represent mean ± SEM $^{****}p < 0.0001$, $^{***}p < 0.001$, $^{**}p < 0.01$, $^{*}p < 0.05$. Two-way ANOVA with Dunnett's multiple comparisons test (compared to VEH) (interaction, F (8, 225) = 8.682; Day, F (2, 225) = 89.66; treatment, F (4, 225) = 18.23). VEH = vehicle (0.9% saline).

immediately after treatment with *R*-MDMA or *R*-MDDMA. We did not observe a head-twitch response (HTR) at any dose tested (Figure 3D), suggesting that both *R*-MDMA and *R*-MDDMA have low hallucinogenic potential. These results are consistent with a recent report suggesting that low doses of R-MDMA (0.1−5 mg/kg) produce negligible effects in the HTR assay.[37] Taken together, these results demonstrate that *R*-MDDMA is likely to have an improved safety profile relative to *R*-MDMA, a compound currently being developed as a safer analogue of *R,S*-MDMA.[38]

R-MDDMA Promotes Fear Extinction

Impaired extinction of fear memories is believed to be a hallmark of PTSD,[39] and both *R,S*-MDMA and *R*-MDMA are known to promote fear extinction in rodents.[22,40] Extinction involves a learning process that attenuates responses to fear memories, and when administered immediately prior to extinction training, *R,S*-MDMA facilitates extinction learning.[18,40] Interestingly, this effect can be achieved if *R,S*-MDMA is administered systemically or directly to either the basolateral amygdala (BLA) or infralimbic cortex (IL).[40]

To compare the effects of *R*-MDMA and *R*-MDDMA on fear extinction learning, we first performed Pavlovian cued fear conditioning by pairing 6 auditory cues with inescapable foot shocks (0.85 mA, 2 s) (Figure 4A). All groups exhibited statistically equivalent levels of freezing prior to compound administration (Figure 4B, Fear Conditioning). The following day, we administered either *R*-MDMA or *R*-MDDMA via intraperitoneal injection and then performed cued fear extinction training 30 min later (Figure 4A). Extinction memory was assessed 24 h later (Figure 4A). We chose to employ doses of 12.5 and 25 mg/kg given that those doses of *R*-MDDMA were well tolerated and did not impact locomotion (Figure 3B).

Both doses of *R*-MDMA given 30 min prior to extinction training caused statistically significant reductions in freezing to the conditioned stimulus during the training session (Figure 4B, FE Training). It is possible that a mild psychostimulant-like effect could be responsible for this reduction in freezing while under the acute effects of the drug; however, these doses did not increase locomotion in the open field (Figure 3B). Alternatively, the acute effects of *R*-MDMA could inhibit the expression of fear responses. In stark contrast, *R*-MDDMA did not impact freezing during fear extinction training (Figure 4B, FE Training). The next day, fear extinction memory was assessed after the compounds had been cleared from the body. Animals treated with either dose of *R*-MDMA or the 12.5 mg/kg dose of *R*-MDDMA exhibited reduced freezing compared to the vehicle control (Figure 4B, Fear Extinction Test). The 25 mg/kg dose of *R*-MDDMA reduced freezing, but the effect was not statistically significant compared to the VEH control. Together, these results suggest that like *R*-MDMA, *R*-MDDMA can produce a sustained reduction in fear memory response when administered immediately prior to fear extinction training.

R-MDDMA Produces Antidepressant-Like Effects

Our lab has previously demonstrated that serotonergic psychedelics and related nonhallucinogenic psychoplastogens can elicit rapid antidepressant-like responses in various rodent behavioral tests including the forced swim test (FST) and tail suspension test (TST).[30,41−43] While these assays have been criticized for their lack of face validity,[44] they exhibit high predictive validity for psychoplastogenic antidepressants when performed >24 h after compound administration. Importantly, the TST has been used to demonstrate that cortical spinogenesis is causally related to the sustained antidepressant-like effects of ketamine[45] and tabernanthalog (TBG).[43] Like the FST, the TST is highly predictive of compounds that possess antidepressant properties in humans and likely relies on activation of mPFC circuits.[46−48]

To assess long-lasting antidepressant-like effects after a single administration, we administered *R*-MDDMA or *R*-MDMA to mice via IP injection and performed a TST 24 h later (Figure 5A). This paradigm reduces the potential for confounding locomotor effects as the mice are no longer under the acute influence of the drugs at the time that immobility is assessed. While the low dose (12.5 mg/kg) failed to produce an antidepressant-like response, the high dose (25 mg/kg) of either *R*-MDDMA or *R*-MDMA reduced immobility to a

https://doi.org/10.1021/acschemneuro.5c00891
ACS Chem. Neurosci. 2026, 17, 1670−1682

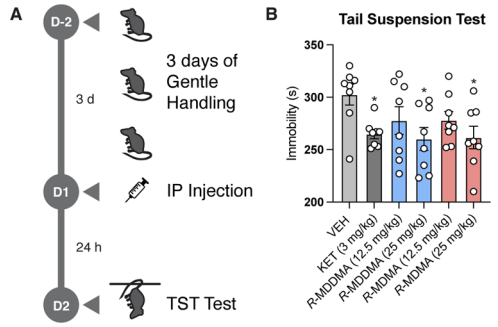

Figure 5. *R*-MDDMA produces an antidepressant-like effect in the TST. (A) Schematic depicting experimental design. Following 3 days of gentle handling, C57BL/6J mice were treated with *R*-MDDMA or *R*-MDMA via intraperitoneal (IP) injections and subjected to a tail suspension test (TST) 24 h later. (B) Both *R*-MDDMA (25 mg/kg) and *R*-MDMA (25 mg/kg) produced a sustained antidepressant-like response, similar to the positive control (KET, 3 mg/kg). $N = 8$ mice (4 males and 4 females) per treatment group. Data represent mean ± SEM $*p < 0.05$. One-way ANOVA with Dunnett's multiple comparisons tests (compared to VEH) ($F(5, 42) = 2.546$). VEH = vehicle (0.9% saline); KET = ketamine.

comparable extent as the positive control ketamine (3 mg/kg) (Figure 5B). To our knowledge, this is the first report demonstrating that *R*-MDMA can produce an antidepressant-like response in rodents, and these data support previous work demonstrating that *R,S*-MDMA can produce antidepressant-like effects when administered to Flinders Sensitive Line rats.[49] It is interesting to note that *R*-MDDMA shares structural similarities to zalsupindole (AAZ-A-154), a nonhallucinogenic psychoplastogen that has demonstrated preclinical efficacy in various assays relevant to depression[50,51] and is currently being developed for the treatment of major depressive disorder.[52]

R-MDDMA Produces Limited Prosocial Effects

Given that both *R,S*-MDMA and *R*-MDMA have demonstrated prosocial effects in rodents,[19,20] we next performed two assays designed to assess the prosocial properties of *R*-MDDMA. First, we performed a 3-chamber social interaction (3-CSI) test 5 min following IP administration of either *R,S*-MDMA or *R*-MDDMA (Figure 6A). A two-way analysis of variance (ANOVA) followed by Dunnett's post hoc test revealed that *R,S*-MDMA increased social interaction compared to the VEH control ($p = 0.0006$) over the course of 25 min. However, neither a low (12.5 mg/kg) nor a high (25 mg/kg) dose of *R*-MDDMA was effective (Figure 6B). Similarly, analyzing the sociability index during the last 10 min of the assay failed to reveal any statistically significant effect of *R*-MDDMA at either dose (Figure 6C). Prior work demonstrated that the largest difference in prosocial behavior following *R,S*-MDMA or vehicle treatment was observed during this epoch.[19]

While the 3-CSI assay assesses a rodent's preference for interacting with a conspecific while under the influence of the drug, it does not inform about whether the animal found this interaction rewarding. To address this aspect of sociability, we performed a social conditioned place preference (sCPP) assay modified from a previous report[53] (Figure 6D). First, we treated mice with a dose of *R,S*-MDMA (7.5 mg/kg) that does not induce a conditioned place preference in the absence of a social stimulus[20] and observed a robust social place preference ($p = 0.02$, Figure 6E). Next, we found that a 20 mg/kg dose of *R*-MDMA trended toward a modest social place preference, though this effect was not statistically significant ($p = 0.05$,

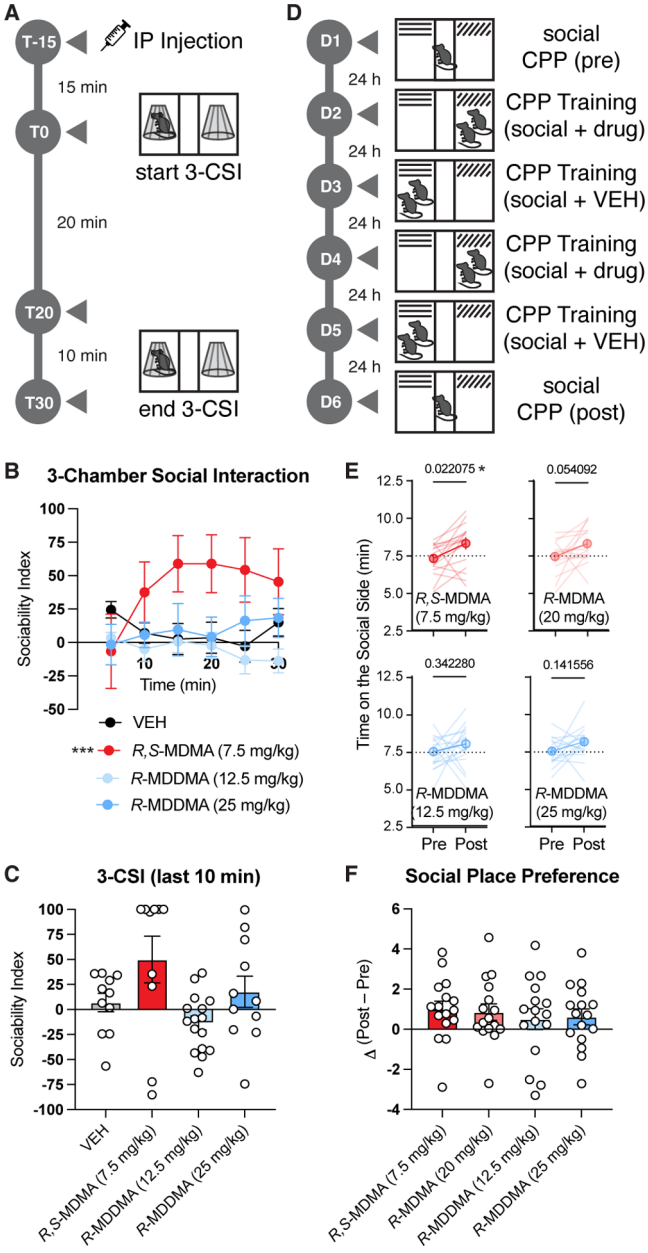

Figure 6. *R*-MDDMA does not produce prosocial effects. (A) Schematic depicting experimental design for the 3-CSI assay. Immediately after drug administration, C57BL/6J mice were confined to the center chamber. After 5 min, they were allowed to freely explore both chambers for an additional 25 min. (B) Sociability index (time in social chamber−time in empty chamber/time in social chamber + time in empty chamber) is reported in 5 min bins. (C) Sociability index during the last 10 min of the 30 min test session is presented. There were no statistical differences between any group and the VEH control. (D) Schematic depicting experimental design for the sCPP assay. (E) During testing, C57BL/6J mice were allowed to freely explore the two chambers for 15 min. A dotted line at 7.5 min represents equal exploration of both chambers with higher and lower values indicating a preference for the social and empty chambers, respectively. Individual *p* values are shown above horizontal bars comparing preferences pre and post training. (F) Changes in time spent in the social chamber following training are shown. There were no statistical differences between any group. Data represent mean ± SEM $****p < 0.0001$, $***p < 0.001$, $**p < 0.01$, $*p < 0.05$. Two-way ANOVA with Dunnett's multiple comparisons test (B, comparing each dose to the VEH control, Interaction, $F(15, 264) =$

https://doi.org/10.1021/acschemneuro.5c00891
ACS Chem. Neurosci. 2026, 17, 1670−1682

Figure 6. continued

1.108, Time, F (5, 264) = 0.4275; Treatment, F (3, 264) = 11.03), a one-way ANOVA with Dunnett's multiple comparisons tests (C, compared to VEH, F (3, 44) = 3.846), two-tailed paired *t* tests (E), or a one-way ANOVA with Tukey's multiple comparisons tests (F, F (3, 60) = 0.2712). VEH = vehicle (0.9% saline).

Figure 6E). Importantly, this dose has been previously shown to induce social interaction in the 3-CSI without producing a conditioned place preference in the absence of a social stimulus.[20] In contrast, *R*-MDDMA did not induce a social place preference at 12.5 mg/kg (p = 0.3, Figure 6E) or 25 mg/kg (p = 0.1, Figure 6E). However, when comparing the change in time spent on the social side before and after training, we found that all the treatments induced a preference on average for the social side with no statistical differences between the groups (Figure 6F). Taken together, these results suggest that *R*-MDDMA produces moderate to no prosocial effects.

While *R,S*-MDMA reliably increases circulating oxytocin (OT), its causal role in the prosocial and therapeutic-like effects of *R,S*-MDMA remain unclear and appears restricted to specific domains. Human studies (including central diabetes insipidus and intranasal OT work), together with rodent antagonist/genetic data, suggests that disrupting OT/vasopressin signaling leaves *R,S*-MDMA-induced social approach and direct interaction largely intact but blunts *R,S*-MDMA-facilitated social reward learning.[54] Thus, OT signaling seems most critical for social reward−learning components of the *R,S*-MDMA-induced state, suggesting that compounds such as *R*-MDDMA that weakly engage this mechanism may still preserve other therapeutic effects that more directly depend on serotonergic signaling.

Mechanistic Studies on *R*-MDDMA

To explain the similarities and differences in the cellular and behavioral effects of *R*-MDMA and *R*-MDDMA, we next performed a series of pharmacological assays. Given that *R*-MDDMA did not produce robust prosocial effects (Figure 6),

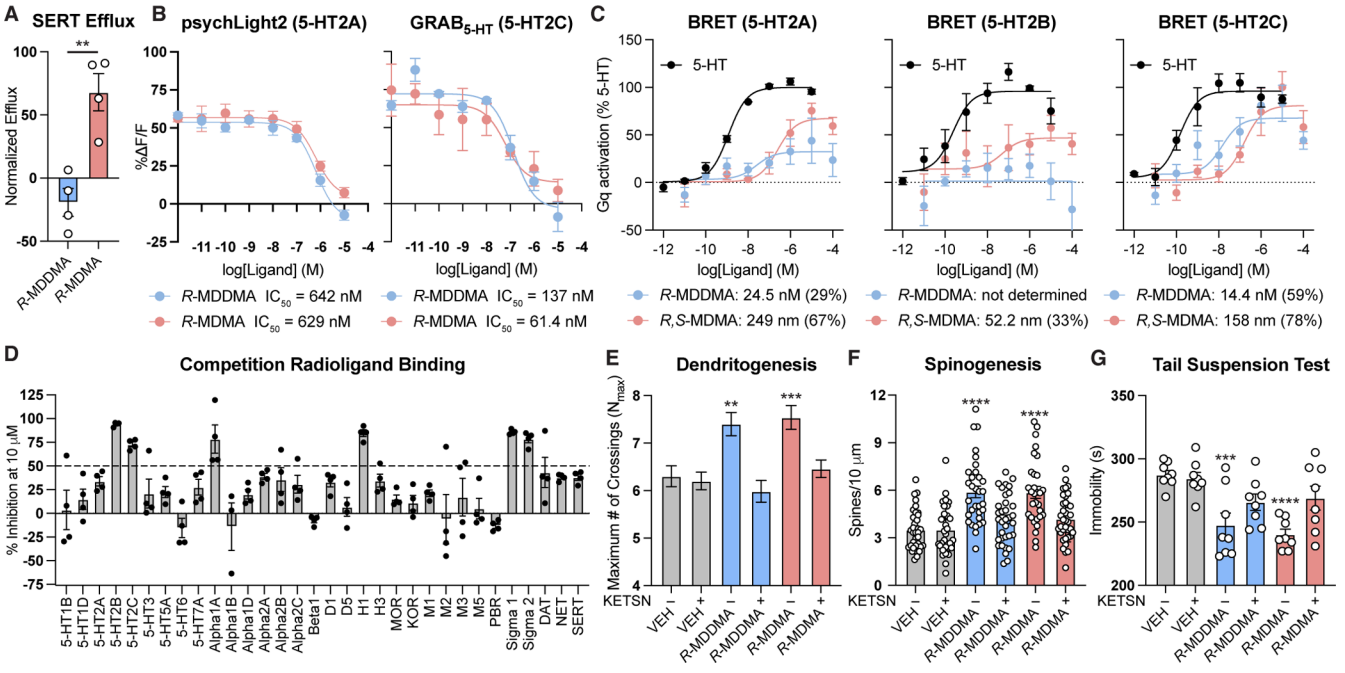

Figure 7. The therapeutic effects of*R*-MDDMA require 5-HT2AR activation. (A) Serotonin release studies were conducted utilizing HEK293T cells expressing SERT and preloaded with [^{3}H]5-HT and indicate that *R*-MDDMA (100 μM) does not induce [^{3}H]5-HT release. Data are normalized to the positive control (100 μM *p*-chloroamphetamine, 100%). (B) 5-HT2-based biosensor assays were conducted in antagonist mode with 100 nM 5-HT added to the media. Both *R*-MDMA and *R*-MDDMA acted as moderately potent antagonists at 5-HT2A and 5-HT2C receptors. (C) Potency (EC_{50}) and efficacy (E_{max}) of Gq activation was assessed using BRET-based methods in HEK293T cells transiently expressing 5-HT2A, 5-HT2B, or 5-HT2C receptors. Data represent well and plate averages across 4 experimental replicates (i.e., independent cultures) and are baseline corrected and normalized to the serotonin response. (D) Competition radioligand binding studies were conducted by the Psychoactive Drug Screening Program (PDSP, https://pdspdb.unc.edu/pdspweb/).[61] Data represent mean ± SEM from 4 replicates. All assays were conducted using a single concentration of *R*-MDDMA (10 μM). Inhibition >50% at 10 μM (dotted line) was deemed meaningful. (E) Cortical neurons (DIV6) were treated with *R*-MDMA (1 μM) or *R*-MDDMA (1 μM) for 72 h. Both *R*-MDMA and *R*-MDDMA increased dendritic arborization relative to the vehicle control, and this effect was blocked by KETSN (10 μM). Maximal number of crossings (N_{max}) from Sholl plots (N = 56−74 neurons from two independent cultures) are shown. (F) Cortical neurons (DIV15) were treated for 24 h with *R*-MDMA or *R*-MDDMA (1 μM). Both *R*-MDMA and *R*-MDDMA increased dendritic spine density relative to the vehicle control, and this effect was blocked by KETSN (10 μM) (N = 30−37 neurons from two independent cultures. Note: data for treatment−KETSN are reproduced from Figure 2E). (G) Following 3 d of gentle handling, C57BL/6J mice were pretreated with VEH or KETSN (4 mg/kg, IP) 10 min prior to receiving IP administration of *R*-MDMA (25 mg/kg) or *R*-MDDMA (25 mg/kg). Animals were subjected to a tail suspension test (TST) 24 h later. N = 8 mice (4 males and 4 females) per treatment group. The sustained antidepressant-like responses of *R*-MDMA and *R*-MDDMA were blocked by KETSN. Data represent mean ± SEM ****p < 0.0001, ***p < 0.001, **p < 0.01, *p < 0.05 for the indicated comparison following Welch's t-test (A) or as compared to the vehicle control following a one-way ANOVA with Dunnett's multiple comparison test (E, F (5, 395) = 8.730; F, F (5, 196) = 14.17; G, F (5, 42) = 7.868). VEH = vehicle (0.1% DMSO); KETSN = ketanserin.

https://doi.org/10.1021/acschemneuro.5c00891
ACS Chem. Neurosci. 2026, 17, 1670−1682

we first assessed its ability to promote serotonin release from SERT-expressing HEK293T cells preloaded with [^{3}H]5-HT. Previously, we have shown that *R,S*-MDMA facilitates serotonin release in these assays.[55,56] As expected, *R*-MDDMA (100 μM) failed to induce 5-HT release while *R*-MDMA produced a large response at the same concentration (Figure 7A). Our data suggest that 5-HT release following treatment with *R,S*-MDDMA[29] is likely mediated by the *S*-enantiomer.

Given that *R,S*-MDMA has been reported to be a weak and/or partial agonist of 5-HT2A and 5-HT2C receptors in BRET-based assays of Gα activation,[57] and 5-HT2 receptors have been implicated in its neuroplasticity-promoting properties,[25] we next tested *R*-MDMA and *R*-MDDMA in assays utilizing cpGFP-based conformational biosensors of 5-HT2 receptors.[50,58] We used psychLight2 and GRAB$_{5\text{-HT}}$ to probe the effects of these compounds at 5-HT2A and 5-HT2C receptors, respectively. Following stimulation with 5-HT (100 nM), we observed concentration-dependent decreases in biosensor signals, consistent with the effects of partial agonists or antagonists (Figure 7B). Potencies ranged from 61−642 nM and were comparable between *R*-MDMA and *R*-MDDMA (Figure 7B).

Next, we performed BRET-based assays to directly assess the ability of *R*-MDDMA and *R,S*-MDMA to activate Gq following 5-HT2 receptor stimulation (Figure 7C).[59] We found that *R*-MDDMA was a relatively potent partial agonist of 5-HT2A receptors (EC_{50} = 25 nM, E_{max} = 29%) with lower efficacy than *R,S*-MDMA (67%). At 5-HT2C receptors, both *R,S*-MDMA and *R*-MDDMA produced higher maximal efficacies (78% and 59%, respectively). Strikingly, and in stark contrast to *R,S*-MDMA, *R*-MDDMA did not activate 5-HT2B receptors at any concentration. This latter point is important considering that 5-HT2B receptor agonism is well-known to be a risk factor for inducing cardiac valvulopathy.[60]

We complemented these targeted functional assays with competition radioligand binding studies to assess the selectivity of *R*-MDDMA across a panel of >30 targets relevant to central nervous system function (Figure 7D). Besides the 5-HT2 family of receptors, *R*-MDDMA only exhibited substantial binding affinities for α1 adrenergic, H1 receptors, and σ receptors. Notably, *R*-MDDMA did not exhibit high affinity for any of the monoamine transporters including SERT.

Because *R*-MDMA and *R*-MDDMA bind to and directly activate 5-HT2A and 5-HT2C receptors, we next assessed the involvement of these receptors in the ability of these compounds to promote cortical neuron growth and structural plasticity. We pretreated immature (DIV6) and mature (DIV15) cortical cultures with *R*-MDMA (1 μM) or *R*-MDDMA (1 μM) in the presence or absence of the 5-HT2 antagonist KETSN (10 μM) and assessed dendritic arborization and spinogenesis, respectively. Both *R*-MDMA and *R*-MDDMA promoted increased dendritic branching measured via Sholl analysis (Figure 7E) as well as spinogenesis (Figure 7F). Importantly, both of these effects on structural neuroplasticity were abrogated by pretreatment with KETSN (Figure 7E,F), suggesting that 5-HT2 signaling is involved in the neuroplasticity-promoting effects of both compounds.

Previous work has demonstrated that dendritic spine growth in the PFC following 5-HT2A receptor activation is critical for the sustained antidepressant-like effects of the nonhallucinogenic psychoplastogen TBG in the TST.[43] Therefore, we pretreated mice with either VEH or KETSN (4 mg/kg, IP) before administering *R*-MDMA (25 mg/kg, IP) or *R*-MDDMA (25 mg/kg, IP). Just as we observed previously, both compounds produced a robust antidepressant-like effect 24 h after administration. However, this effect was blocked by KETSN pretreatment, suggesting that 5-HT2 activation is essential (Figure 7G).

CONCLUSION

The mechanisms by which *R,S*-MDMA produces beneficial effects in the clinic are complex,[62] which has led some investigators to pursue close structural analogues in the hope of retaining the high therapeutic potential of *R,S*-MDMA while improving on its suboptimal safety and scalability profile.[63−65] In fact, a recent phase 2 clinical trial demonstrated that methylone—a close structural congener of *R,S*-MDMA that promotes cortical neuron growth—produced large therapeutic effects in patients with PTSD without any associated psychotherapy.[66] We took a different approach to developing a safer *R,S*-MDMA analogue involving the methylation of the *R*-enantiomer for several reasons. First, *R*-MDMA has been previously shown to possess an improved safety profile compared to the *S*-enantiomer.[20−22] Second, *N*-methylation of tryptamines improves their ability to promote cortical neuron growth through stimulation of intracellular 5-HT2A receptors.[30] This small structural modification did not negatively impact the 5-HT2A-dependent psychoplastogenic effects of *R*-MDDMA, nor did it impair its ability to promote fear extinction or produce sustained antidepressant-like effects. However, *N*-methylation of *R*-MDMA did further improve its safety profile. Though many compounds containing *N,N*-dimethylamino substituents are at least partially demethylated in vivo, the extent of any *R*-MDDMA demethylation to produce *R*-MDMA must be relatively low given that the two compounds exhibit very distinct profiles in assays measuring locomotion and thigmotaxis. Taken together, our work implicates direct 5-HT2 receptor activation in the psychoplastogenic effects of *R*-MDDMA and adds to the growing list of nonhallucinogenic psychoplastogens.[32,41,51,65,67,68]

METHODS

Data Analysis and Statistics

Treatments were randomized, and data were analyzed by experimenters blinded to treatment conditions. Statistical analyses were performed using GraphPad Prism (version 10.5.0) unless noted otherwise. All comparisons were planned prior to performing each experiment. Sample sizes were determined based on literature reports, pilot experiments, or power analysis. Both sexes were used, but studies were not powered to detect sex differences. Thus, data from male and female animals were combined. No data were excluded.

Drugs

For cell culture experiments, the vehicle was a 0.1% (agonist studies) or 0.2% (antagonist studies) molecular biology grade dimethyl sulfoxide (DMSO, Sigma-Aldrich). For in vivo experiments, the vehicle was USP grade saline (0.9%). The hemifumarate salt of *R*-3,4-methyl enedioxy methamphetamine (2:1, R-MDMA:fumaric acid) and the fumarate salt of *R*-3,4-methylenedioxy-*N,N*-dimethylamphetamine (1:1, R-MDDMA:fumaric acid) was synthesized in-house as reported previously, and judged to be analytically pure on the basis of nuclear magnetic resonance (NMR) and liquid chromatography−mass spectrometry (LC−MS) data.[50] Other chemicals were purchased from commercial sources as follows: ketamine hydrochloride (KET, Fagron), ketanserin tartrate (KTSN, Alfa Aesar), 5-[1,2-^{3}H[N]]-hydroxytryptamine creatinine sulfate ([^{3}H]5-HT, Perki-

https://doi.org/10.1021/acschemneuro.5c00891
ACS Chem. Neurosci. 2026, 17, 1670−1682

nElmer), (±)-*para*-chloroamphetamine hydrochloride (PCA, Sigma-Aldrich).

Animals

All experimental procedures involving animals were approved by the Institutional Animal Care and Use Committees at the University of California, Davis (IACUC protocols 18955, 19319, 20655, 22375, 21030, 19229, and 22795) or Stanford University (IACUC protocol 10322) and adhered to the principles described in the NIH Guide for the Care and Use of Laboratory Animals. UC Davis and Stanford University are accredited by the Association for Assessment and Accreditation of Laboratory Animal Care International (AAALAC). Timed pregnancy (E18) Sprague−Dawley rats were obtained from Charles River Laboratories (Wilmington, MA, USA). Mice (C57BL/6J) were obtained from Jackson Laboratory (Stock No. 000664) and were approximately 9−13 weeks old at the time of the experiments. Mice were group housed (2−5 mice per cage) under controlled temperature in a 12 h light/dark cycle (7:00 AM to 7:00 PM) with access to food and water ad libitum.

Dendritogenesis Experiments

Culturing, immunostaining, and data analysis was performed as previously described[32] with the exception that there was no media change after treatments and compounds were left in the culture media for 72 h. The vehicle (VEH) and positive controls were DMSO (0.1%) and ketamine (10 μM), respectively. For blocking experiments, antagonists were added 30 min prior to addition of agonists in 10-fold excess. Experiments were performed in duplicate with plates prepared using neurons obtained from independent pregnant dams.

Spinogenesis Experiments

Spinogenesis experiments were performed as previously described[25] with the exception that cells were treated at DIV14 and fixed 24 h after treatment on DIV15. The images were obtained using a Nikon HCA confocal microscope a with a 100*x*/NA 1.45 oil objective. The vehicle (VEH) and positive controls were DMSO (0.1%) and ketamine (10 μM), respectively. For blocking experiments, antagonists were added 30 min prior to addition of agonists in 10-fold excess. Experiments were performed in duplicate with plates prepared using neurons obtained from independent pregnant dams.

Body Temperature Assessment, Novelty-Induced Locomotion, and Head-Twitch Response

The head-twitch response assay was performed as described previously[32] using both male and female C57BL/6J mice. Before administering the compound, the baseline temperatures of the mice were measured using an IR thermometer as previously described.[69] Dose responses of *R*-MDMA and *R*-MDDMA (12.5, 25, 50 mg/kg) were conducted via IP administration using 0.9% saline as the vehicle (5 mL/kg). Immediately after treatment, the animals were placed in a 40 cm × 40 cm arena for 30 min where their locomotor activity was assessed using AnyMaze automated tracking software. Their behavior was also video recorded and scored offline for head twitches by a blinded observer. Upon completion of the novelty induced locomotion assay, their body temperature was measured at the 30 min time point. The mice were then transferred to a holding cage with treatment-matched cage mates and their temperatures were measured at the 90- and 120 min time points.

Fear Extinction

Male and female mice were exposed to cued fear conditioning on day one, fear extinction training on day two and extinction testing on day three. Each mouse was handled for approximately 1 min by a male experimenter for three consecutive days leading up to the first day of behavioral testing. All experiments were carried out by the same male experimenter. Mice were allowed to habituate to the behavior room for 1 h before beginning the experiment. Approximately 15 min before starting the experiment, mice were separated out into individual holding cages. Cued fear conditioning consisted of six pairings of a conditioned stimulus (CS) auditory cue (80 dB white noise, 15 s) and a coterminating unconditioned stimulus (US) foot shock (0.85 mA and 2 s), each spaced 1.5 min apart. The fear conditioning apparatus (Med Associates model # MED-VFC2-SCT-R) consisted of a 30.5 cm × 24.1 cm × 21 cm internal soundproof chamber, with metal grated floors, an infrared camera, a sound generator, and a light source. Mice were initially placed in the conditioning apparatus and the first 1.5 min were stimulus free. After the last shock, the animals remained in the chambers for an additional 2 min before being returned to their home cages. During fear conditioning, the apparatus was illuminated to 100 l*x* and did not contain any additional odor cues. Freezing responses for fear conditioning (Day 1) are presented as the percentage of time spent freezing during the last 1.5 min after the last shock. The apparatus was cleaned with 70% EtOH in between trials. On day two, animals were separated into individual holding cages and were administered either VEH (0.9% USP saline), *R*-MDMA (12.5 or 25 mg/kg), or *R*-MDDMA (12.5 or 25 mg/kg) via IP injection (5 mL/kg) 30 min prior to being placed in the fear extinction context. Cued fear memory was assessed by exposing the animals to a novel context (lights off, A-frame insert, smooth plastic floor inserts, additional vanilla odor) for 2 min prior to 16 presentations of auditory cues (80 dB white noise, 15 s) spaced 15 s apart. Freezing responses for cue testing (Day 2 and 3) are presented as the percentage of time spent freezing during the white noise presentations. The procedure was repeated on Day 3 in the absence of drug. Freezing behavior was scored using Med Associates Video Freeze software v2.25 (motion threshold = 100 au, detection method = linear, minimum freeze duration = 15 frames, which is equal to a 0.5 s freeze). The apparatus was cleaned with scented Sani-cloth gemicidal disposable cloths (PDI, Q89072) on days two and three to create a distinct odor in context B.

Tail Suspension Test (TST)

Male and female C57/BL6J mice were obtained from Jackson Lab and housed in a UC Davis vivarium. Each mouse was handled for approximately 1 min by a male experimenter for three consecutive days leading up to the first day of behavioral testing. All experiments were carried out by the same male experimenter. Mice were allowed to habituate to the behavior room for 1 h before beginning the experiment. All TST sessions were performed between the hours of 08:00 and 13:00. On Day 1, mice were administered VEH (0.9% USP saline), ketamine hydrochloride 3 mg/kg (Fagron), *R*-MDMA (12.5 or 15 mg/kg), or *R*-MDDMA (12.5 or 25 mg/kg) via IP injection (5 mL/kg). For blocking experiments, 4 mg/kg of ketanserin tartrate (Alfa Aesar, J62798) was administered via IP injection 10 min prior to compound administration. On Day 2, animals were subjected to a tail suspension test. Animals were suspended from their tails approximately 16 cm from the top of the apparatus and 25 cm from the bottom of the apparatus. Behavior was video recorded for 6 min and analyzed later by an experimenter blinded to treatment conditions. Immobility was defined as the amount of time spent not struggling or attempting to generate momentum and was scored for the entire 6 min period.

3-Chamber Social Interaction (3-CSI)

The three-chamber apparatus (length, 72 cm; width, 23 cm; height, 25 cm) was built in-house using 0.635 cm-thick sheets of clear extruded acrylic for walls, white Komatex for floors, and black barrier walls (TAP Plastics). The apparatus consisted of two outer chambers (28 cm by 23 cm) connected by a center chamber (16 cm by 23 cm). On day one, test mice were habituated to the arena containing two, 10 cm-diameter, wire mesh, empty, inverted cups placed in the center of the two outer chambers for 10 min. Conspecific mice were also habituated to the mesh cups for 10 min. On day two, a conspecific mouse (age- and sex-matched, wild-type, unfamiliar) was placed into one of the wire mesh cups (social stimulus). Test mice were injected with *R*-MDDMA (12.5 or 25 mg/kg, IP), *R*-MDMA (20 mg/kg, IP), *R,S*-MDMA (7.5 mg/kg, IP), or vehicle (saline, IP) and placed into the center chamber. After a 15 min habituation, the barriers of the center chamber were raised, and the test mouse was allowed to explore freely during a 30 min session. Between experimental sessions, the cups and the three-chamber apparatus were wiped down with 70% ethanol. The placement of the conspecific mouse was counterbalanced across sessions. The cups used to hold mice were regularly

https://doi.org/10.1021/acschemneuro.5c00891
ACS Chem. Neurosci. 2026, 17, 1670−1682

rotated to minimize the effect of residual scents. Video was acquired by a computer-controlled ceiling-mounted digital camera and analyzed offline using Biobserve tracking software (BiobserveGmbH). Mice were excluded from further analysis if they either failed to explore both cup and cup mouse chambers or if they spent more than 75% of allotted time in the center chamber, not exploring either cup. We have previously found that the prosocial effect of *R*,*S*-MDMA in the 3-CSI test maximally separates from vehicle injections in the final 10 min of a 30 min assay.[19] The amount of time spent in the "social" and "nonsocial" outer chambers was automatically scored by Biobserve. Sociability was calculated as ((time in social side−time in empty side)/(time in social side + time in empty side))*100.

Social Conditioned Place Preference (sCPP)

Two equal-sized compartments were created within a testing chamber (Med Associates, Fairfax, VT). The chamber was an acryclic box, internal dimensions of 28 cm × 28 cm × 20 cm. Each compartment had a distinct floor, either clear, textured acrylic ("A" side) or smooth, black acrylic ("B" side). Left/right positioning of the floors was alternated between conditioning chambers. Conditioning experiments involving *R*,*S*-MDMA, *R*-MDMA and *R*-MDDMA took place over 6 consecutive days. Day 1, Pretest: For 15 min, the mouse had free access to both compartments, separated by a clear acrylic divider with a 7 cm diameter hole for passage. Baseline preference was measured as the amount of time spent per side. Mice were pseudorandomly allocated to either the "A" or "B" side for drug conditioning such that the net baseline preference within an experimental group was as close to 7.5 min as possible and equal numbers of mice were assigned to "A" and "B" sides. Day 2, first conditioning day: For 30 min, 2 conspecific mice were sequestered to either "A" or "B" side by a solid transparent divider, starting 15 min after both mice received an IP injection of test drug. Day 3, second conditioning day: The experiment was performed as on Day 2 except both mice received saline injections and were sequestered in the opposite compartment ("A" or "B"). Day 4 and 5 repeated the procedures of Day 2 and 3, respectively. Day 6, post-test: the experiment was performed as on Day 1. Mouse movement was tracked by an array of infrared beam break counters, recorded using Med Associates software, and analyzed offline.

SERT Efflux Experiments

Cells (HEK293T, AATCCRL-3216; mycoplasma free) were grown in complete media consisting of DMEM high glucose-pyruvate (Gibco, #11995065), 1% Penicillin−Streptomycin (Giboco, # 5140122), and 10% fetal bovine serum (Gibco # 26140079). The day prior to the experiment, cells were plated in 24-well plates at a density of 150,000 cells/well and concurrently transfected using Lipofectamine 3000 Transfection Reagent (Invitrogen catalog, #L3000001) according to the manufacturer's protocol. Cells were transfected with hSERT-N1-pEYFP (Addgene, #70105) or a GFP control plasmid (Lonza, pmaxGFP vector). The next day the wells were washed (1 × 500 μL) with 1X Hank's Balanced Salt Solution (HBSS) supplemented with 2 mM $MgCl_2$ and 2 mM $CaCl_2$ (ThermoFisher, 14025092) and the plate was placed on a 37 °C water bath for the remainder of the experiment. 250 μL of HBSS containing 10 nM 5-[1,2-^{3}H[N]]-hydroxytryptamine creatinine sulfate (NET498001MC, Lot: 2902700) was added to the wells and incubated for 15 min, allowing uptake into SERT-expressing HEK293T cells. Uptake was terminated by aspiration of wells followed by washes (3 × 500 μL) with HBSS. Efflux was initiated by adding 250 μL of compound solutions with 0.2% DMSO as the vehicle control, 100 μM PCA (Sigma-Aldrich, C9635-1G) as the positive control, 100 μM−10 pM *R*-MDMA, or 100 μM−10 pM *R*-MDDMA in HBSS for 15 min. Media (200 μL) was collected from each well and placed into a scintillation vial containing 1 mL PerkinElmer Ultima Gold scintillation cocktail to serve as the efflux fraction. The wells were washed (3 × 500 μL) with HBSS and then cells were lysed for 10 min by adding 250 μL radioimmunoprecipitation assay (RIPA) buffer (50 mM Tris HCl, 150 mM NaCl, 1% NP-40, 0.5% sodium deoxycholate, 0.1% SDS, pH 8) to each well. Cells were lysed with a P1000 pipet using the RIPA buffer in the well and all contents of the well were collected into separate scintillation vials containing 1 mL PerkinElmer Ultima Gold scintillation cocktail to serve as the intracellular fraction. An additional 250 μL of RIPA buffer was added to each well and then transferred to the intracellular fraction vials. Scintillation vials were mixed by inverting and incubating overnight at room temperature. Radioactivity in the form of disintegrations per minute (DPM) was determined the following day with the use of a Beckman LS 6000 liquid scintillation counter. The efflux fraction counts were corrected by *a* factor of 1.25 to account for the 50 μL remaining in each well (DPM * 250 μL total/200 μL collected). Using the DPM for each compound, bar graphs were reported as efflux fraction/(efflux fraction + intracellular fraction) and then normalized to the vehicle control and positive control with the vehicle set at 0% and 100 μM PCA positive control set at 100%. The GFP control cells were checked to ensure radioactivity was below background levels.

Biosensor Experiments

For experiments using PSYLI2 cells[50] (HEK293T cell line stably expressing psychLight2; mycoplasma free) cells were plated at 8.0 × 10^4 cells/well in poly-D-lysine coated glass bottom 96-well plates (P96-1.5H-N, Cellvis) in complete media (DMEM-high glucose-pyruvate, Gibco, #11995065; 1% penicillin−streptomycin, Giboco, # 5140122; 10% fetal bovine serum, Gibco # 26140079) and returned to the incubator. For experiments using the $GRAB_{5\text{-}HT}$ sensor,[58] HEK293T (AATCCRL-3216; mycoplasma free) cells were grown in complete media. The day prior to the experiment, cells were plated at 8.0 × 10^4 cells/well in poly-D-lysine coated glass bottom 96-well plates (P96-1.5H-N, Cellvis) and concurrently transfected using Lipofectamine 3000 Transfection Reagent (Invitrogen catalog, #L3000001) according to the manufacturer's protocol. Cells were transfected with the pCMV_GRAB5-HT1.0 biosensor (subcloned from Addgene, #140552). The next day, plates were washed three times with warm HBSS supplemented with 2 mM $MgCl_2$ and 2 mM $CaCl_2$. Next, 50 μL HBSS was added to the wells of the assay plate and a baseline scan was performed using a CellInsight CX7 HCA Platform (ThermoFisher, CX7A1110) connected to an onstage incubator for live cell imaging (ThermoFisher, NX7LIVE001) at 40*x* with nine ROIs taken per well using an arbitrary ROI pattern for each well with no bias to location and no overlap of the ROIs (exposure = 400 ms, LED power = 100%). A 100 μM 5-HT stock in DMSO was diluted in HBSS to a 200 nM solution. Then, 50 μL of 200 nM 5-HT was added to the wells to achieve a final concentration of 100 nM 5-HT (total dilution = 1:1000). After a 5 min incubation, the plate was scanned. Immediately prior to reimaging, 10 mM stock solutions of drugs in DMSO were diluted in HBSS to 20 μM and distributed across an empty 96-well treatment plate in triplicate following a randomized plate map. Serial 1:10 dilutions were performed in the treatment plate to generate a concentration response. Following this, a 10 mM drug stock of *R*-MDMA or *R*-MDDMA in DMSO was diluted in HBSS to a 20 μM solution, and 100 μL of the 20 μM drug solution was added to the wells to achieve a final concentration of 10 μM (total dilution = 1:1000). After a 5 min incubation, the plate was rescanned. Once imaging was complete, the images were exported and processed through a custom Python script to obtain average $\Delta F/F$ values for each treatment (https://github.com/moagonzalez/OlsonLab/blob/main/PsychLightV3_Clean.txt). Next, $\Delta F/F$ values for each treatment were fitted to a nonlinear regression of agonist vs response (three parameter) using GraphPad Prism. Responses were normalized to the positive control (100 nM 5-HT) set as 100% and the average of the 1 pM concentration response between both treatments on each graph set as 0%. An 8-point concentration response was performed for each compound.

BRET-Based Assays of 5-HT2 Receptor Activation

HEK293T cells were seeded into T75 flasks and incubated in DMEM +10% FBS at 37 °C and 5% CO_2 until 80% confluent. Transfection complexes were prepared at component ratios of 1200 μL optiMEM:12 μg total plasmid mix:36 μL TransIT-293 reagent per flask, where the total plasmid mix was either a 1:1:1:1 mixture of 5-HT2A, Gγ9-GFP2, Gβ3, Gαq-rLuc8, a 1:1:1:1 mixture of 5-HT2B, Gγ9-GFP2, Gβ3, Gαq-rLuc8, or a 1:2:2:2 mixture of 5-HT2C, Gγ9-

https://doi.org/10.1021/acschemneuro.5c00891
ACS Chem. Neurosci. 2026, 17, 1670−1682

GFP2, Gβ3, Gαq-rLuc8 (Addgene[59]). Media was replaced with 10 mL of fresh prewarmed DMEM +10% FBS and 1.2 mL transfection complex was added. Flasks were incubated for 24 h at 37 °C and 5% CO_2. Transfected cells were then seeded into 50 μg/mL poly-D-lysine-coated white optical bottom 96-well Nunclon Delta plates at a seeding density of 60,000 cells/well. Plates were incubated in 200 μL of DMEM +10% dialyzed FBS for 24 h at 37 °C and 5% CO_2 prior to performing the assay. Next, plates were washed 3 × 100 μL HBSS and replaced with 80 μL/well of Live Cell Imaging Solution (Invitrogen). The assay was then carried out similarly to a previous report,[67] whereby cells were treated with 10 μL/well of compound stock solutions to produce varying concentrations of serotonin (5-HT), *R,S*-MDMA, or *R*-MDDMA (final solutions contained 0.1% DMSO) and incubated for 55 min at 37 °C and 5% CO_2 prior to addition of 10 μL/well 10*x* RLuc substrate Prolume Purple (1.33 μM final concentration; 1:150 dilution into Live Cell Imaging Solution from 2 mM stock solution in NanoFuel Solvent; NanoLight Technology). Then, 5 min after addition of substrate, bioluminescence donor emission (410−480 nm) and BRET acceptor GFP emission (515 nm) were measured on a Pherastar FSX (BMG Labtech, USA) at 37 °C every 2 min for 8 min using a BRET2 optic module. The average of four consecutive reads were used to calculate BRET2 ratios and transformed to a concentration−response curve baseline-corrected measure of Gαq protein activation, normalized to the maximal response of 5-HT on the same plate. Experiments were performed in quadruplicate and responses on a given day were averaged to yield biological replicates. Grouped data represents $N = 4$ independent experiments.

AUTHOR INFORMATION

Corresponding Author

David E. Olson − *Institute for Psychedelics and Neurotherapeutics, University of California, Davis, Davis, California 95616, United States; Department of Chemistry, University of California, Davis, Davis, California 95616, United States; Department of Biochemistry & Molecular Medicine, School of Medicine, University of California, Davis, Sacramento, California 95817, United States; Center for Neuroscience, University of California, Davis, Davis, California 95618, United States;* orcid.org/0000-0002-4517-0543; Email: deolson@ucdavis.edu

Authors

Maxemiliano V. Vargas − *Institute for Psychedelics and Neurotherapeutics, University of California, Davis, Davis, California 95616, United States; Neuroscience Graduate Program, University of California, Davis, Davis, California 95618, United States*

Cassandra J. Hatzipantelis − *Institute for Psychedelics and Neurotherapeutics, University of California, Davis, Davis, California 95616, United States; Department of Chemistry, University of California, Davis, Davis, California 95616, United States; Department of Biochemistry & Molecular Medicine, School of Medicine, University of California, Davis, Sacramento, California 95817, United States;* orcid.org/0000-0001-5376-7887

Lee E. Dunlap − *Institute for Psychedelics and Neurotherapeutics, University of California, Davis, Davis, California 95616, United States; Chemistry and Chemical Biology Graduate Program, University of California, Davis, Davis, California 95616, United States*

Robert J. Tombari − *Institute for Psychedelics and Neurotherapeutics, University of California, Davis, Davis, California 95616, United States; Chemistry and Chemical Biology Graduate Program, University of California, Davis, Davis, California 95616, United States;* orcid.org/0000-0002-6561-8181

Arabo A. Avanes − *Institute for Psychedelics and Neurotherapeutics, University of California, Davis, Davis, California 95616, United States; Biochemistry, Molecular, Cellular, and Developmental Biology Graduate Program, University of California, Davis, Davis, California 95616, United States*

Sam Vaillancourt − *Department of Anesthesiology, Perioperative and Pain Medicine, Stanford University School of Medicine, Stanford, California 94305, United States; Department of Psychiatry and Behavioral Sciences, Stanford University, Stanford, California 94305, United States;* orcid.org/0009-0007-2220-9998

Pierre Llorach − *Department of Anesthesiology, Perioperative and Pain Medicine, Stanford University School of Medicine, Stanford, California 94305, United States; Department of Psychiatry and Behavioral Sciences, Stanford University, Stanford, California 94305, United States*

Juliana S. Salgado − *Department of Anesthesiology, Perioperative and Pain Medicine, Stanford University School of Medicine, Stanford, California 94305, United States*

Boris D. Heifets − *Department of Anesthesiology, Perioperative and Pain Medicine, Stanford University School of Medicine, Stanford, California 94305, United States; Department of Psychiatry and Behavioral Sciences, Stanford University, Stanford, California 94305, United States*

Complete contact information is available at: https://pubs.acs.org/10.1021/acschemneuro.5c00891

Author Contributions

MVV performed all the in vitro cellular experiments as well as the body temperature, novelty-induced locomotion, head-twitch response, fear extinction, and tail suspension test assays. CJH performed all BRET-based assays of 5-HT2 receptor activation and assisted with the analysis of competition radioligand binding assay data. LED synthesized *R*-MDMA and *R*-MDDMA used for these studies. RJT and AAA performed and analyzed the SERT efflux experiments with assistance from MVV. SV and PL performed the 3-chamber social interaction and social conditioned place preference assays. BDH supervised the 3-chamber social interaction and social conditioned place preference assays. DEO conceived and supervised the project. DEO and MVV wrote the manuscript with input from all authors.

Notes

The authors declare the following competing financial interest(s): D.E.O. is a co-founder of Delix Therapeutics, Inc., serves as the Chief Innovation Officer and Head of the Scientific Advisory Board, and has sponsored research agreements with Delix Therapeutics. B.D.H. is a co-founder of Ocellaris, Inc., is on the scientific advisory boards of Journey Clinical and Osmind, and is a paid consultant to Arcadia Medicine, Inc, Tactogen, LLC, and Vida Ventures, LLC.

ACKNOWLEDGMENTS

We would like to thank Van La for assisting with the synthesis of compounds, Hannah Saeger from subcloning the $GRAB_{5\text{-}HT}$ biosensor, and Calvin Ly for assisting with pilot neuritogenesis studies. This work was supported by funds from the Camille and Henry Dreyfus Foundation (DEO), the Pershing Square Foundation (DEO), and funds from an anonymous donation.

This project used the Biological Analysis Core of the UC Davis MIND Institute Intellectual and Development Disabilities Research Center (U54 HD079125). The Nikon High Content Analysis Spinning Disk Confocal microscope used in this study was purchased using NIH Shared Instrumentation Grant 1S10OD019980-01A1. We thank the MCB Light Microscopy Imaging Facility, which is a UC Davis Campus Core Research Facility, for the use of this microscope. Receptor binding data were generously provided by the National Institute of Mental Health's Psychoactive Drug Screening Program, Contract # 75N95023C00021 (NIMH PDSP). The NIMH PDSP is Directed by Bryan L. Roth MD, PhD at the University of North Carolina at Chapel Hill and Project Officer Jamie Driscoll at NIMH, Bethesda MD, USA.

REFERENCES

(1) Dunlap, L. E.; Andrews, A. M.; Olson, D. E. Dark Classics in Chemical Neuroscience: 3,4-Methylenedioxymethamphetamine. *ACS Chem. Neurosci.* **2018**, *9* (10), 2408−2427.
(2) Shulgin, A. T. The background and chemistry of MDMA. *J. Psychoactive Drugs.* **1986**, *18* (4), 291−304.
(3) Greer, G.; Tolbert, R. Subjective reports of the effects of MDMA in a clinical setting. *J. Psychoactive Drugs.* **1986**, *18* (4), 319−327.
(4) Young, M. B.; Andero, R.; Ressler, K. J.; Howell, L. L. 3,4-Methylenedioxymethamphetamine facilitates fear extinction learning. *Transl. Psychiatry* **2015**, *5* (9), No. e634.
(5) Nardou, R.; Lewis, E. M.; Rothhaas, R.; Xu, R.; Yang, A.; Boyden, E.; Dölen, G. Oxytocin-dependent reopening of a social reward learning critical period with MDMA. *Nature.* **2019**, *569* (7754), 116−120.
(6) Walsh, J. J.; Christoffel, D. J.; Heifets, B. D.; Ben-Dor, G. A.; Selimbeyoglu, A.; Hung, L. W.; Deisseroth, K.; Malenka, R. C. 5-HT release in nucleus accumbens rescues social deficits in mouse autism model. *Nature.* **2018**, *560* (7720), 589−594.
(7) Walsh, J. J.; Llorach, P.; Cardozo Pinto, D. F.; Wenderski, W.; Christoffel, D. J.; Salgado, J. S.; Heifets, B. D.; Crabtree, G. R.; Malenka, R. C. Systemic enhancement of serotonin signaling reverses social deficits in multiple mouse models for ASD. *Neuropsychopharmacology* **2021**, *46* (11), 2000−2010.
(8) Rein, B.; Raymond, K.; Boustani, C.; Tuy, S.; Zhang, J.; St Laurent, R.; Pomrenze, M. B.; Boroon, P.; Heifets, B.; Smith, M.; Malenka, R. C. MDMA enhances empathy-like behaviors in mice via 5-HT release in the nucleus accumbens. *Sci. Adv.* **2024**, *10* (17), No. eadl6554.
(9) Mithoefer, M. C.; Wagner, M. T.; Mithoefer, A. T.; Jerome, L.; Doblin, R. The safety and efficacy of {±}3,4-methylenedioxymethamphetamine-assisted psychotherapy in subjects with chronic, treatment-resistant posttraumatic stress disorder: the first randomized controlled pilot study. *J. Psychopharmacol.* **2011**, *25* (4), 439−452.
(10) Mitchell, J. M.; Bogenschutz, M.; Lilienstein, A.; Harrison, C.; Kleiman, S.; Parker-Guilbert, K.; Ot'alora G, M.; Garas, W.; Paleos, C.; Gorman, I.; Nicholas, C.; Mithoefer, M.; Carlin, S.; Poulter, B.; Mithoefer, A.; Quevedo, S.; Wells, G.; Klaire, S. S.; van der Kolk, B.; Tzarfaty, K.; Amiaz, R.; Worthy, R.; Shannon, S.; Woolley, J. D.; Marta, C.; Gelfand, Y.; Hapke, E.; Amar, S.; Wallach, Y.; Brown, R.; Hamilton, S.; Wang, J. B.; Coker, A.; Matthews, R.; de Boer, A.; Yazar-Klosinski, B.; Emerson, A.; Doblin, R. MDMA-assisted therapy for severe PTSD: a randomized, double-blind, placebo-controlled phase 3 study. *Nat. Med.* **2021**, *27* (6), 1025−1033.
(11) Mitchell, J. M.; Ot'alora G, M.; van der Kolk, B.; Shannon, S.; Bogenschutz, M.; Gelfand, Y.; Paleos, C.; Nicholas, C. R.; Quevedo, S.; Balliett, B.; Hamilton, S.; Mithoefer, M.; Kleiman, S.; Parker-Guilbert, K.; Tzarfaty, K.; Harrison, C.; de Boer, A.; Doblin, R.; Yazar-Klosinski, B.; et al. MAPP2 Study Collaborator Group. MDMA-assisted therapy for moderate to severe PTSD: a randomized, placebo-controlled phase 3 trial. *Nat. Med.* **2023**, *29* (10), 2473−2480.
(12) Wilkinson, S. T.; Sanacora, G. Issues in Clinical Trial Design-Lessons From the FDA's Rejection of MDMA. *JAMA Psychiatry* **2025**, *82* (6), 545−546.
(13) Kvam, T. M.; Goksøyr, I. W.; Stewart, L. H.; Repantis, D.; Røssberg, J. I.; Andreassen, O. A. Study protocol for "MDMA-assisted therapy as a treatment for major depressive disorder: A proof of principle study". *Front Psychiatry.* **2022**, *13*, 954388.
(14) Green, A. R.; Mechan, A. O.; Elliott, J. M.; O'Shea, E.; Colado, M. I. The pharmacology and clinical pharmacology of 3,4-methylenedioxymethamphetamine (MDMA, "ecstasy"). *Pharmacol. Rev.* **2003**, *55* (3), 463−508.
(15) Brennan, K. A.; Carati, C.; Lea, R. A.; Fitzmaurice, P. S.; Schenk, S. Effect of D1-like and D2-like receptor antagonists on methamphetamine and 3,4-methylenedioxymethamphetamine self-administration in rats. *Behav. Pharmacol.* **2009**, *20* (8), 688−694.
(16) Vidal-Infer, A.; Roger-Sánchez, C.; Daza-Losada, M.; Aguilar, M. A.; Miñarro, J.; Rodríguez-Arias, M. Role of the dopaminergic system in the acquisition, expression and reinstatement of MDMA-induced conditioned place preference in adolescent mice. *PLoS One* **2012**, *7* (8), No. e43107.
(17) Beardsley, P. M.; Balster, R. L.; Harris, L. S. Self-administration of methylenedioxymethamphetamine (MDMA) by rhesus monkeys. *Drug Alcohol Depend.* **1986**, *18* (2), 149−157.
(18) Young, M. B.; Norrholm, S. D.; Khoury, L. M.; Jovanovic, T.; Rauch, S. A. M.; Reiff, C. M.; Dunlop, B. W.; Rothbaum, B. O.; Howell, L. L. Inhibition of serotonin transporters disrupts the enhancement of fear memory extinction by 3,4-methylenedioxymethamphetamine (MDMA). *Psychopharmacology (Berl).* **2017**, *234* (19), 2883−2895.
(19) Heifets, B. D.; Salgado, J. S.; Taylor, M. D.; Hoerbelt, P.; Cardozo Pinto, D. F.; Steinberg, E. E.; Walsh, J. J.; Sze, J. Y.; Malenka, R. C. Distinct neural mechanisms for the prosocial and rewarding properties of MDMA. *Sci. Transl. Med.* **2019**, *11* (522), No. eaaw6435.
(20) Pomrenze, M. B.; Vaillancourt, S.; Salgado, J. S.; Raymond, K. B.; Llorach, P.; Sacai, H.; Rijsketic, D. R.; Hietamies, T. M.; Touponse, G. C.; Cardozo Pinto, D. F.; Rastegar, Z.; Casey, A. B.; Eshel, N.; Malenka, R. C.; Heifets, B. D. 5-HT2C receptors in the nucleus accumbens constrain the rewarding effects of MDMA. *Mol. Psychiatry* **2025**, *30* (11), 5405−5416.
(21) Pitts, E. G.; Curry, D. W.; Hampshire, K. N.; Young, M. B.; Howell, L. L. (±)-MDMA and its enantiomers: potential therapeutic advantages of R(−)-MDMA. *Psychopharmacology (Berl).* **2018**, *235* (2), 377−392.
(22) Curry, D. W.; Young, M. B.; Tran, A. N.; Daoud, G. E.; Howell, L. L. Separating the agony from ecstasy: R(−)-3,4-methylenedioxymethamphetamine has prosocial and therapeutic-like effects without signs of neurotoxicity in mice. *Neuropharmacology.* **2018**, *128*, 196−206.
(23) Olson, D. E. Psychoplastogens: A Promising Class of Plasticity-Promoting Neurotherapeutics. *J. Exp. Neurosci.* **2018**, *12*, 1179069518800508.
(24) Vargas, M. V.; Meyer, R.; Avanes, A. A.; Rus, M.; Olson, D. E. Psychedelics and Other Psychoplastogens for Treating Mental Illness. *Front Psychiatry.* **2021**, *12*, 727117.
(25) Ly, C.; Greb, A. C.; Cameron, L. P.; Wong, J. M.; Barragan, E. V.; Wilson, P. C.; Burbach, K. F.; Soltanzadeh Zarandi, S.; Sood, A.; Paddy, M. R.; Duim, W. C.; Dennis, M. Y.; McAllister, A. K.; Ori-McKenney, K. M.; Gray, J. A.; Olson, D. E. Psychedelics Promote Structural and Functional Neural Plasticity. *Cell Rep.* **2018**, *23* (11), 3170−3182.
(26) Martínez-Turrillas, R.; Moyano, S.; Del Río, J.; Frechilla, D. Differential effects of 3,4-methylenedioxymethamphetamine (MDMA, "ecstasy") on BDNF mRNA expression in rat frontal cortex and hippocampus. *Neurosci. Lett.* **2006**, *402* (1−2), 126−130.
(27) Peters, J.; Dieppa-Perea, L. M.; Melendez, L. M.; Quirk, G. J. Induction of fear extinction with hippocampal-infralimbic BDNF. *Science.* **2010**, *328* (5983), 1288−1290.
(28) Alexander, A. T. S.; Shulgin, A. *PiHKAL: A Chemical Love Story*; Transform Press 1991; pp725−726.

https://doi.org/10.1021/acschemneuro.5c00891
ACS Chem. Neurosci. 2026, 17, 1670−1682

(29) Sandtner, W.; Stockner, T.; Hasenhuetl, P. S.; Partilla, J. S.; Seddik, A.; Zhang, Y. W.; Cao, J.; Holy, M.; Steinkellner, T.; Rudnick, G.; Baumann, M. H.; Ecker, G. F.; Newman, A. H.; Sitte, H. H. Binding Mode Selection Determines the Action of Ecstasy Homologs at Monoamine Transporters. *Mol. Pharmacol.* **2016**, *89* (1), 165−175.
(30) Vargas, M. V.; Dunlap, L. E.; Dong, C.; Carter, S. J.; Tombari, R. J.; Jami, S. A.; Cameron, L. P.; Patel, S. D.; Hennessey, J. J.; Saeger, H. N.; McCorvy, J. D.; Gray, J. A.; Tian, L.; Olson, D. E. Psychedelics promote neuroplasticity through the activation of intracellular 5-HT2A receptors. *Science.* **2023**, *379* (6633), 700−706.
(31) Zhou, F. C.; Sari, Y.; Zhang, J. K. Expression of serotonin transporter protein in developing rat brain. *Brain Res. Dev Brain Res.* **2000**, *119* (1), 33−45.
(32) Dunlap, L. E.; Azinfar, A.; Ly, C.; Cameron, L. P.; Viswanathan, J.; Tombari, R. J.; Myers-Turnbull, D.; Taylor, J. C.; Grodzki, A. C.; Lein, P. J.; Kokel, D.; Olson, D. E. Identification of Psychoplastogenic *N*,*N*-Dimethylaminoisotryptamine (isoDMT) Analogues through Structure-Activity Relationship Studies. *J. Med. Chem.* **2020**, *63* (3), 1142−1155.
(33) Callaway, C. W.; Clark, R. F. Hyperthermia in psychostimulant overdose. *Ann. Emerg. Med.* **1994**, *24* (1), 68−76.
(34) Wise, R. A. Dopamine, learning and motivation. *Nat. Rev. Neurosci.* **2004**, *5* (6), 483−494.
(35) Ikemoto, S. Dopamine reward circuitry: two projection systems from the ventral midbrain to the nucleus accumbens-olfactory tubercle complex. *Brain Res. Rev.* **2007**, *56* (1), 27−78.
(36) Peroutka, S. J.; Newman, H.; Harris, H. Subjective effects of 3,4-methylenedioxymethamphetamine in recreational users. *Neuropsychopharmacology* **1988**, *1* (4), 273−277.
(37) Gaines-Smith, M. C.; Silverman, J. M.; Fiorillo, M.; Younkin, J.; Moore, K. N.; Maltman, J. L.; de la Fuente Revenga, M.; Wolstenholme, J. T.; Glennon, R. A.; Dukat, M.; González-Maeso, J. Stereoselective, sex-dependent 5-HT2A receptor modulation of cortical plasticity by MDMA in mice. *Neuropsychopharmacology* **2026**.
(38) Straumann, I.; Avedisian, I.; Klaiber, A.; Varghese, N.; Eckert, A.; Rudin, D.; Luethi, D.; Liechti, M. E. Acute effects of R-MDMA, S-MDMA, and racemic MDMA in a randomized double-blind cross-over trial in healthy participants. *Neuropsychopharmacology* **2025**, *50* (2), 362−371.
(39) Rothbaum, B. O.; Davis, M. Applying learning principles to the treatment of post-trauma reactions. *Ann. N.Y. Acad. Sci.* **2003**, *1008*, 112−121.
(40) Young, M. B.; Andero, R.; Ressler, K. J.; Howell, L. L. 3,4-Methylenedioxymethamphetamine facilitates fear extinction learning. *Transl. Psychiatry* **2015**, *5* (9), No. e634.
(41) Cameron, L. P.; Patel, S. D.; Vargas, M. V.; Barragan, E. V.; Saeger, H. N.; Warren, H. T.; Chow, W. L.; Gray, J. A.; Olson, D. E. 5-HT2ARs Mediate Therapeutic Behavioral Effects of Psychedelic Tryptamines. *ACS Chem. Neurosci.* **2023**, *14* (3), 351−358.
(42) Cameron, L. P.; Tombari, R. J.; Lu, J.; Pell, A. J.; Hurley, Z. Q.; Ehinger, Y.; Vargas, M. V.; McCarroll, M. N.; Taylor, J. C.; Myers-Turnbull, D.; Liu, T.; Yaghoobi, B.; Laskowski, L. J.; Anderson, E. I.; Zhang, G.; Viswanathan, J.; Brown, B. M.; Tjia, M.; Dunlap, L. E.; Rabow, Z. T.; Fiehn, O.; Wulff, H.; McCorvy, J. D.; Lein, P. J.; Kokel, D.; Ron, D.; Peters, J.; Zuo, Y.; Olson, D. E. A non-hallucinogenic psychedelic analogue with therapeutic potential. *Nature.* **2021**, *589* (7842), 474−479.
(43) Aarrestad, I. K.; Cameron, L. P.; Fenton, E. M.; Casey, A. B.; Rijsketic, D. R.; Patel, S. D.; Sambyal, R.; Johnson, S. B.; Ly, C.; Viswanathan, J.; Barragan, E. V.; Lozano, S. A.; Seban, N.; Hu, H.; Powell, N. A.; Chytil, M.; Meyer, R.; Rose, D.; Hempel, C.; Olson, E.; Hansen, H. D.; Madsen, C. A.; Knudsen, G. M.; Redd, C.; Wheeler, D. G.; Guanzon, N.; Muir, J.; Hennessey, J. J.; Quon, G.; McCorvy, J. D.; Gandhi, S. P.; Rasmussen, K.; Liston, C.; Gray, J. A.; Heifets, B. D.; Nord, A. S.; Kim, C. K.; Olson, D. E. The psychoplastogen tabernanthalog induces neuroplasticity without proximate immediate early gene activation. *Nat. Neurosci.* **2025**, *28*, 1919−1931.
(44) Trunnell, E. R.; Baines, J.; Farghali, S.; Jackson, T.; Jayne, K.; Smith, R.; Stibbe, T. The need for guidance in antidepressant drug development: Revisiting the role of the forced swim test and tail suspension test. *Regul. Toxicol. Pharmacol.* **2024**, *151*, 105666.
(45) Moda-Sava, R. N.; Murdock, M. H.; Parekh, P. K.; Fetcho, R. N.; Huang, B. S.; Huynh, T. N.; Witztum, J.; Shaver, D. C.; Rosenthal, D. L.; Alway, E. J.; Lopez, K.; Meng, Y.; Nellissen, L.; Grosenick, L.; Milner, T. A.; Deisseroth, K.; Bito, H.; Kasai, H.; Liston, C. Sustained rescue of prefrontal circuit dysfunction by antidepressant-induced spine formation. *Science.* **2019**, *364* (6436), No. eaat8078.
(46) Can, A.; Dao, D. T.; Terrillion, C. E.; Piantadosi, S. C.; Bhat, S.; Gould, T. D. The tail suspension test. *J. Vis Exp.* **2012**, No. 59, No. e3769.
(47) Cryan, J. F.; Mombereau, C.; Vassout, A. The tail suspension test as a model for assessing antidepressant activity: review of pharmacological and genetic studies in mice. *Neurosci. Biobehav. Rev.* **2005**, *29* (4−5), 571−625.
(48) Warden, M. R.; Selimbeyoglu, A.; Mirzabekov, J. J.; Lo, M.; Thompson, K. R.; Kim, S.-Y.; Adhikari, A.; Tye, K. M.; Frank, L. M.; Deisseroth, K. A prefrontal cortex-brainstem neuronal projection that controls response to behavioural challenge. *Nature.* **2012**, *492* (7429), 428−432.
(49) Majumder, I.; White, J. M.; Irvine, R. J. Antidepressant-like effects of 3,4-methylenedioxymethamphetamine in an animal model of depression. *Behav. Pharmacol.* **2011**, *22* (8), 758−765.
(50) Dong, C.; Ly, C.; Dunlap, L. E.; Vargas, M. V.; Sun, J.; Hwang, I.-W.; Azinfar, A.; Oh, W. C.; Wetsel, W. C.; Olson, D. E.; Tian, L. Psychedelic-inspired drug discovery using an engineered biosensor. *Cell.* **2021**, *184* (10), 2779−2792 e18.
(51) Agrawal, R.; Gillie, D.; Mungenast, A.; Chytil, M.; Engel, S.; Wu, M. C.; Rasmussen, K.; Salinas, E.; Olson, D. E. Zalsupindole is a non-dissociative, non-hallucinogenic neuroplastogen. *ACS Chem. Neurosci.* **2025**, *16*, 4388.
(52) Koenig, A.; van der Aa, L.; Pelletier, N.; Patat, A.; Viardot, G.; Olson, D.; Rasmussen, K.; van der Heijden, K.; Borghans, L.; Doll, R. J.; Jacobs, G.; Salinas, E. ACNP 63rd Annual Meeting: Poster Abstracts P163. *Neuropsychopharmacology* **2024**, *49*, 65−235.
(53) Ramos, L.; Hicks, C.; Caminer, A.; Goodwin, J.; McGregor, I. S. Oxytocin and MDMA ('Ecstasy') enhance social reward in rats. *Psychopharmacology (Berl)* **2015**, *232* (14), 2631−2641.
(54) Casey, A. B.; Heifets, B. D. History, pharmacology and therapeutic mechanisms of 3,4-methylenedioxymethamphetamine (MDMA). *Br. J. Pharmacol.* **2025**, bph.70225.
(55) Avanes, A. A.; Warren, H. T.; Senthil, A.; Olson, D. E. Pharmacological Evaluation of Tropane Analogues at the Serotonin Transporter. *ACS Chem. Neurosci.* **2025**, *16* (17), 3354−3363.
(56) Iyer, R. N.; Favela, D.; Domokos, A.; Zhang, G.; Avanes, A. A.; Carter, S. J.; Basargin, A. G.; Davis, A. R.; Tantillo, D. J.; Olson, D. E. Efficient and modular synthesis of ibogaine and related alkaloids. *Nat. Chem.* **2025**, *17* (3), 412−420.
(57) Jain, M. K.; Gumpper, R. H.; Slocum, S. T.; Schmitz, G. P.; Madsen, J. S.; Tummino, T. A.; Suomivuori, C.-M.; Huang, X.-P.; Shub, L.; DiBerto, J. F.; Kim, K.; DeLeon, C.; Krumm, B. E.; Fay, J. F.; Keiser, M.; Hauser, A. S.; Dror, R. O.; Shoichet, B.; Gloriam, D. E.; Nichols, D. E.; Roth, B. L. The polypharmacology of psychedelics reveals multiple targets for potential therapeutics. *Neuron* **2025**, *113* (19), 3129−3142 e9.
(58) Wan, J.; Peng, W.; Li, X.; Qian, T.; Song, K.; Zeng, J.; Deng, F.; Hao, S.; Feng, J.; Zhang, P.; Zhang, Y.; Zou, J.; Pan, S.; Shin, M.; Venton, B. J.; Zhu, J. J.; Jing, M.; Xu, M.; Li, Y. A genetically encoded sensor for measuring serotonin dynamics. *Nat. Neurosci.* **2021**, *24* (5), 746−752.
(59) Olsen, R. H. J.; DiBerto, J. F.; English, J. G.; Glaudin, A. M.; Krumm, B. E.; Slocum, S. T.; Che, T.; Gavin, A. C.; McCorvy, J. D.; Roth, B. L.; Strachan, R. T. TRUPATH, an open-source biosensor platform for interrogating the GPCR transducerome. *Nat. Chem. Biol.* **2020**, *16*, 841−849.
(60) Rothman, R. B.; Baumann, M. H.; Savage, J. E.; Rauser, L.; McBride, A.; Hufeisen, S. J.; Roth, B. L. Evidence for possible involvement of 5-HT(2B) receptors in the cardiac valvulopathy

associated with fenfluramine and other serotonergic medications. *Circulation* **2000**, *102*, 2836−2841.
(61) Besnard, J.; Ruda, G. F.; Setola, V.; Abecassis, K.; Rodriguiz, R. M.; Huang, X. P.; Norval, S.; Sassano, M. F.; Shin, A. I.; Webster, L. A.; Simeons, F. R.; Stojanovski, L.; Prat, A.; Seidah, N. G.; Constam, D. B.; Bickerton, G. R.; Read, K. D.; Wetsel, W. C.; Gilbert, I. H.; Roth, B. L.; Hopkins, A. L. Automated design of ligands to polypharmacological profiles. *Nature* **2012**, *492*, 215−220.
(62) Heifets, B. D.; Olson, D. E. Therapeutic mechanisms of psychedelics and entactogens. *Neuropsychopharmacology* **2024**, *49* (1), 104−118.
(63) Johnson, C. B.; Walther, D.; Baggott, M. J.; Baker, L. E.; Baumann, M. H. Novel Benzofuran Derivatives Induce Monoamine Release and Substitute for the Discriminative Stimulus Effects of 3,4-Methylenedioxymethamphetamine. *J. Pharmacol. Exp. Ther.* **2024**, *391* (1), 22−29.
(64) Alberto-Silva, A. S.; Hemmer, S.; Bock, H. A.; da Silva, L. A.; Scott, K. R.; Kastner, N.; Bhatt, M.; Niello, M.; Jäntsch, K.; Kudlacek, O.; Bossi, E.; Stockner, T.; Meyer, M. R.; McCorvy, J. D.; Brandt, S. D.; Kavanagh, P.; Sitte, H. H. Bioisosteric analogs of MDMA: Improving the pharmacological profile? *J. Neurochem.* **2024**, *168* (9), 2022−2042.
(65) Warner-Schmidt, J.; Stogniew, M.; Mandell, B.; Kelmendi, B. Methylone promotes neurite outgrowth and has long-lasting effects on fear extinction learning. *Neuropsychopharmacology* **2025**, *51*, 631−640.
(66) Jones, A.; Warner-Schmidt, J.; Kwak, H.; Stogniew, M.; Mandell, B.; Ching, T. H. W.; Stein, M. B.; Kelmendi, B. Efficacy and Safety of the Neuroplastogen TSND-201 for the Treatment of PTSD: A Randomized Clinical Trial. *JAMA Psychiatry* **2026**, No. e254625.
(67) Tuck, J. R.; Dunlap, L. E.; Khatib, Y. A.; Hatzipantelis, C. J.; Weiser Novak, S.; Rahn, R. M.; Davis, A. R.; Mosswood, A.; Vernier, A. M. M.; Fenton, E. M.; Aarrestad, I. K.; Tombari, R. J.; Carter, S. J.; Deane, Z.; Wang, Y.; Sheridan, A.; Gonzalez, M. A.; Avanes, A. A.; Powell, N. A.; Chytil, M.; Engel, S.; Fettinger, J. C.; Jenkins, A. R.; Carlezon, W. A., Jr; Nord, A. S.; Kangas, B. D.; Rasmussen, K.; Liston, C.; Manor, U.; Olson, D. E. Molecular design of a therapeutic LSD analogue with reduced hallucinogenic potential. *Proc. Natl. Acad. Sci. U. S. A.* **2025**, *122* (16), No. e2416106122.
(68) Lewis, V.; Bonniwell, E. M.; Lanham, J. K.; Ghaffari, A.; Sheshbaradaran, H.; Cao, A. B.; Calkins, M. M.; Bautista-Carro, M. A.; Arsenault, E.; Telfer, A.; Taghavi-Abkuh, F. F.; Malcolm, N. J.; El Sayegh, F.; Abizaid, A.; Schmid, Y.; Morton, K.; Halberstadt, A. L.; Aguilar-Valles, A.; McCorvy, J. D. A non-hallucinogenic LSD analog with therapeutic potential for mood disorders. *Cell Rep.* **2023**, *42* (3), 112203.
(69) Kawakami, Y.; Sielski, R.; Kawakami, T. Mouse Body Temperature Measurement Using Infrared Thermometer During Passive Systemic Anaphylaxis and Food Allergy Evaluation. *J. Vis Exp.* **2018**, No. 139, 58391.

https://doi.org/10.1021/acschemneuro.5c00891
ACS Chem. Neurosci. 2026, 17, 1670−1682